μ distortions or running: A guaranteed discovery from CMB spectrometry

Giovanni Cabass,[1] Alessandro Melchiorri,[1] and Enrico Pajer[2]

[1]*Physics Department and INFN, Università di Roma "La Sapienza", P.le Aldo Moro 2, 00185 Rome, Italy*
[2]*Institute for Theoretical Physics and Center for Extreme Matter and Emergent Phenomena,*
Utrecht University, Leuvenlaan 4, 3584 CE Utrecht, The Netherlands

We discuss the implications of a PIXIE-like experiment, which would measure μ-type spectral distortions of the cosmic microwave background (CMB) at a level of $\sigma_\mu = (1/n) \times 10^{-8}$, with $n \geq 1$ representing an improved sensitivity (e.g. $n = 10$ corresponds to PRISM). Using Planck data and considering the six-parameter ΛCDM model, we compute the posterior for $\mu_8 \equiv \mu \times 10^8$ and find $\mu_8 = 1.57^{+0.11}_{-0.13}$ (68% C.L.). This becomes $\mu_8 = 1.28^{+0.30}_{-0.52}$ (68% C.L.) when the running α_s of the spectral index is included. We point out that a sensitivity of about $3 \times$ PIXIE implies a *guaranteed discovery*: μ distortion is detected or $\alpha_s \geq 0$ is excluded (both at 95% C.L. or higher). This threshold sensitivity sets a clear benchmark for CMB spectrometry. For a combined analysis of PIXIE and current Planck data, we discuss the improvement on measurements of the tilt n_s and the running α_s and the dependence on the choice of the pivot. A fiducial running of $\alpha_s = -0.01$ (close to the Planck best fit) leads to a detection of negative running at 2σ for $5 \times$ PIXIE. A fiducial running of $\alpha_s = -0.02$, still compatible with Planck, requires $3 \times$ PIXIE to rule out $\alpha_s = 0$ (at 95% C.L.). We propose a convenient and compact visualization of the improving constraints on the tilt, running and tensor-to-scalar ratio.

I. INTRODUCTION

The recent measurements of cosmic microwave background (CMB) anisotropies made by the Planck satellite experiment [1] have provided, once again, a spectacular confirmation of the ΛCDM cosmological model and determined its parameters with an impressive accuracy. Also, numerous new ground-based or balloon-borne CMB telescopes are currently gathering data or under development. Moreover, several proposals for a new satellite experiment like PIXIE [2], PRISM [3,4], CORE [5], and LiteBIRD [6] are under discussion.

In summary, two main lines of investigation are currently pursued: CMB polarization and spectral distortions. Improving current measurements of CMB polarization is partially motivated by the inflationary paradigm. As it is well known, the simplest models of inflation predict a nearly scale-invariant (red-tilted) spectrum of primordial scalar perturbations, in perfect agreement with the latest experimental evidence. Inflation also predicts a stochastic background of gravitational waves: a discovery of this background (e.g. through measurements of CMB B-mode polarization [7,8]) with a tensor-to-scalar ratio $r \sim 10^{-2}$ would correspond to inflation occurring at the grand unified theory (GUT) scale. Planned and/or proposed CMB experiments could detect this background, and measure the tensor-to-scalar ratio $r \sim 0.01 \times (E_{\text{inflation}}/10^{16} \text{ GeV})^4$ with a relative error of order 10^{-2}, if inflation occurs at these energies [9,10]. This would be a spectacular confirmation of the inflationary theory. However, the energy scale of

inflation could be orders of magnitude lower than the GUT scale. In this case, the stochastic background would be out of the reach of upcoming or planned experiments.

On the other hand, CMB μ-type spectral distortions are an unavoidable prediction of the ΛCDM model, since they are generated by the damping of primordial fluctuations [11,12] with an amplitude of order $\mu = \mathcal{O}(10^{-8})$ (for this reason, it will be useful to define the parameter $\mu_8 \equiv \mu \times 10^8$, that will be used in the rest of the paper).

While a measurement of CMB spectral distortions could shed light on several aspects of physics beyond ΛCDM such as, e.g., gravitino decay [13], cosmic strings [14], magnetic fields [15], hidden photons [16], and dark matter interactions [17], just to name a few, we stress that spectral distortions could provide significant information on inflation through the contribution coming from primordial perturbations [18–22].

Indeed, in a typical inflationary model, the spectral index n_s of scalar perturbations is expected to have a small (and often negative) running, of order $|\alpha_s| \sim (1 - n_s)^2$ [23–25]. State-of-the art CMB observations by the Planck experiment [1,26] are fully compatible with an exact power-law spectrum of primordial fluctuations $P_\zeta(k)$, with $\alpha_s = -0.006 \pm 0.007$ at 68% C.L. (Planck TT, TE, EE + lowP data set). A more than tenfold improvement in sensitivity is therefore needed to reach the typical slow-roll values with CMB experiments. However, CMB anisotropies can probe $P_\zeta(k)$ only up to $k \approx 0.1 \text{ Mpc}^{-1}$, since at shorter scales primordial anisotropies are washed away by Silk damping [27–29] and foregrounds become dominant. There is, then, a limit in the

range of multipoles that we can use to test the scale dependence of the power spectrum.[1] Moreover, CMB measurements will soon be limited by cosmic variance: recent analyses have shown that for upcoming experiments (CORE+ or CMB Stage IV), which are close to being cosmic variance limited, one can expect $\sigma_{\alpha_s} \approx 10^{-3}$ [31–33].

The CMB μ-type spectral distortion is sensitive to the amount of scalar power up to k of order 10^4 Mpc^{-1} because of the damping of acoustic modes. The strong lever arm makes this observable an ideal probe to improve the bounds on the running from large-scale CMB anisotropies. In addition, the cosmic variance of the μ monopole and of the higher multipoles is minuscule (see Ref. [34] for a discussion). With a sufficiently broad frequency coverage, instrumental noise will be the main source of uncertainty for the foreseeable future, leaving ample room for improvements.

In this context, we address several questions:

 (i) Is there a benchmark sensitivity for CMB spectrometry, i.e. which should be the target of the next-generation experiments? How can we design an experiment to ensure a discovery even in the absence of a detection?
 (ii) What sensitivity to the spectrum is needed to detect μ distortions when accounting for the prior knowledge from Planck?
 (iii) How much will a joint analysis of large-scale CMB anisotropies and CMB spectral distortion strengthen the bounds on the running? How does this quantitatively depend on the improvement over PIXIE sensitivity?[2]

To articulate the answers to these questions, we consider the following three fiducial cosmologies:

 (i) A ΛCDM cosmology with zero running: the best fit for the μ amplitude, in this case, is of order $\mu_8 = 1.6$. We stress that for the sensitivities considered in this work, this fiducial is indistinguishable from models with running of order $(1 - n_s)^2$, such as typical slow-roll models.
 (ii) A fiducial spectral distortion amplitude $\mu_8^{(\text{fid})}$ equal to the best fit of the Planck analysis for the ΛCDM + α_s model, i.e. $\mu_8^{(\text{fid})} = 1.06$. This value of μ is roughly correspondent to what one obtains for a running $\alpha_s = -0.01$ which is close to the mean value predicted by current Planck data.
 (iii) $\alpha_s^{(\text{fid})} = -0.02$ (corresponding to $\mu_8 = 0.73$), at the edge of the 2σ bounds of Planck. We note that it is possible to obtain such large negative runnings in some models of single-field inflation like, e.g.,

extra-dimensional versions of natural inflation [35,36] or recent developments in axion monodromy inflation [37–39].

The paper is organized as follows. After a brief review of photon thermodynamics in the early Universe and of distortions from Silk damping (Sec. II), we compute the μ-distortion parameter allowed by current Planck bounds for a ΛCDM and ΛCDM + α_s model (Sec. III). We then analyze what a PIXIE-like mission will be able to say about the running, given these posteriors for μ. The discussion is divided into three sections. We start with the predicted bounds on μ distortions from current Planck data (Sec. III). We proceed with a Fisher analysis (Sec. IV), discussing also the optimal choice of pivot scale for a combined study of CMB anisotropies and spectral distortions. The Markov chain Monte Carlo (MCMC) analysis and forecasts are carried out in Sec. V. Finally, Sec. VI studies the implications of these results for single-clock slow-roll inflation, and we draw our conclusions in Sec. VII.

II. PHOTON THERMODYNAMICS

At very early times, for redshifts larger than $z_{\text{dC}} \approx 2 \times 10^6$, processes like double Compton scattering and bremsstrahlung are very efficient and maintain thermodynamic equilibrium: any perturbation to the system is thermalized and the spectrum of the CMB is given to very high accuracy by a black body. At later times the photon number is effectively frozen, since photons can be created at low frequencies by elastic Compton scattering but their re-scattering at high frequencies via double Compton scattering and bremsstrahlung is not efficient due to the expansion of the Universe [11,40–44].

The end result is a Bose-Einstein distribution $1/(e^{x+\mu(x)} - 1)$ ($x \equiv h\nu/k_B T$) with chemical potential μ. Since photons can still be created at low frequencies, μ will not be exactly frequency independent: it can be approximated as $\mu_\infty \exp(-x_c/x)$, with $x_c \approx 5 \times 10^{-3}$. However, no planned/proposed experiments will be able to probe such low frequencies: for this reason we will take the chemical potential to be a constant (and drop the subscript ∞).

For a given energy release $d(Q/\rho_\gamma)/dz$, one can write the value of μ as (see Sec. VIII A)

$$\mu(z) = 1.4 \int_z^{z_{\text{dC}}} dz' \frac{d(Q/\rho_\gamma)}{dz'} e^{-\tau_{\text{dC}}(z')}, \tag{1}$$

where the *distortion visibility function* $\tau_{\text{dC}}(z)$ can be approximated as $(z/z_{\text{dC}})^{5/2}$ [11,40–45].

Below redshifts around $z = z_{\mu\text{-}i} \approx 2 \times 10^5$, Compton scattering is not sufficient to maintain a Bose-Einstein spectrum in the presence of energy injection. The distortions generated will then be neither μ type nor y type: they will depend on the redshift at which energy injection occurs [20,43,46], and must be calculated numerically by solving the Boltzmann equation (known as the Kompaneets

---

[1]For this reason, we expect that E-mode polarization will be better, in the long run, at constraining the scale dependence of $P_\zeta(k)$, since C_ℓ^{EE} starts to become damped around $\ell \approx 2500$ (see Ref. [30] for a discussion).

[2]For example the PRISM imager [3,4] corresponds to approximately $10 \times$ PIXIE.

equation [47], when restricted to Compton scattering). Recently, in Refs. [20,46], a set of Green's functions for the computation of these intermediate distortions has been provided[3]: they sample the intermediate photon spectrum $n^{(i)}$ for a energy release $Q_{\mathrm{ref}/\rho_\gamma} = 4 \times 10^{-5}$ in $\mathcal{O}(10^3)$ redshift bins from $z \approx 2 \times 10^5$ to $z \approx 1.5 \times 10^4$. The i-type occupation number, for a generic energy injection history $d(Q/\rho_\gamma)/dz$, will then be computed as [20]

$$
\begin{aligned}
I^{(i)}(\nu) &= \frac{2h\nu^3}{c^2} \sum_{z_k} \frac{n_{z_k}^{(i)}(\nu)}{4 \times 10^{-5}} \frac{d(Q/\rho_\gamma)}{dz}\bigg|_{z_k} \delta z_k \\
&\equiv \frac{2h\nu^3}{c^2} \sum_{z_k} \frac{n_{z_k}^{(i)}(\nu)}{4 \times 10^{-5}} \times \mu_{z_k}^{(i)}.
\end{aligned}
\tag{2}
$$

At redshifts $z \lesssim 1.5 \times 10^4$ elastic Compton scattering is also not efficient enough: there is no kinetic equilibrium and the distortion is of y type. The transition between μ and y distortions can be modeled with a redshift-dependent visibility function [48]. The information on the transition is encoded in the residual r-type distortions. Since r distortions are not degenerate with μ- and y-type distortions (see Sec. VIII B), they can be useful for probing the redshift dependence of different energy release histories [20,49].[4]

The y-type distortions are expected to be dominated by astrophysics at low redshifts (created when the CMB photons are scattered in the clusters of galaxies by hot electrons—the tSZ effect). While this signal is very interesting by itself as a probe of the matter distribution in the Universe [50–52], our goal is studying the contribution due to dissipation of acoustic waves, and so we will marginalize over it in our analysis (see Sec. VIII B).[5]

Additional spectral distortions are the ones created during recombination [45,54] and reionization [45,55,56]. Previous work on recombination spectra has been carried out in Refs. [57–62], and recently the authors of Ref. [54] have shown that spectral distortions from recombination can be computed with high precision. Therefore we are not going to include them in our analysis, assuming they can be subtracted when looking for the primordial signal.

In this work we will not consider these intermediate distortions, and take the transition between the μ and y eras to be instantaneous at a redshift $z_{\mu\text{-}y} \approx 5 \times 10^4$ [12]: in the case of an energy release that does not vary abruptly with redshift, we do not expect the inclusion of r distortions to

---

[3]We refer also to Ref. [48] for an alternate derivation.
[4]As the authors of Ref. [43] have shown, they can be used to put constraints on observables like the lifetime of decaying dark matter particles.
[5]We note that in Ref. [53], the authors carried out this marginalization by taking into account also r distortions: this results in slightly higher μ detection limits, but does not affect the main results of this paper.
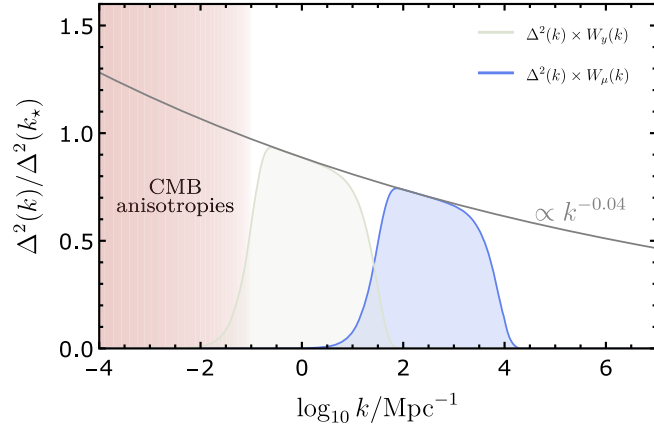
alter significantly the constraints on the parameters describing $d(Q/\rho_\gamma)/dz$. We leave the analysis of their effect on combined CMB anisotropies–CMB distortions forecasts for cosmological parameters for future work (we refer to Refs. [20,49,53] for forecasts involving CMB spectrometry alone).

While there are many nonstandard potential sources of spectral distortions, e.g. decaying or annihilating dark matter particles [13,43,46], a source of heating that is present also in the standard picture is the dissipation of perturbations in the primordial plasma due to Silk damping. Even before recombination, when the tight-coupling approximation holds, photons are random-walking within the plasma with a mean free path $\lambda_{\mathrm{mfp}} = (n_e \sigma_{\mathrm{T}})^{-1}$. In the fluid description, this amounts to anisotropic stresses that induce dissipation. One can compute the (integrated) fractional energy lost by these acoustic waves δ_γ: in the tight-coupling approximation Eq. (1) reduces to [63,64]

$$
\begin{aligned}
\mu &\approx \frac{1.4}{4} \langle \delta_\gamma^2(z,\boldsymbol{x}) \rangle_p \big|_{z_{\mu\text{-}y}}^{z_{\mathrm{dC}}} \\
&\approx 2.3 \int \frac{d\boldsymbol{k}_1 d\boldsymbol{k}_2}{(2\pi)^3} e^{i\boldsymbol{k}_+ \cdot \boldsymbol{x}} \zeta_{\boldsymbol{k}_1} \zeta_{\boldsymbol{k}_2} e^{-(k_1^2+k_2^2)/k_D^2} \big|_{z_{\mu\text{-}y}}^{z_{\mathrm{dC}}},
\end{aligned}
\tag{3}
$$

where $\langle \dots \rangle_p$ indicates the average over a period of oscillation and ζ is the primordial curvature perturbation. The diffusion damping length appearing in the above formula, instead, is given by [27–29]

$$
k_{\mathrm{D}}(z) = \sqrt{\int_z^{+\infty} dz \frac{1+z}{Hn_e\sigma_{\mathrm{T}}} \left[\frac{R^2 + \frac{16}{15}(1+R)}{6(1+R)^2} \right]}.
\tag{4}
$$

If we consider the ensemble average of μ, we see that it is equal to the log-integral of the primordial power spectrum multiplied by a window function

$$
W_\mu(k) = 2.3 e^{-2k^2/k_D^2} \big|_{z_{\mu\text{-}y}}^{z_{\mathrm{dC}}}.
\tag{5}
$$

Since the tight-coupling approximation is very accurate at redshifts much before recombination we expect this to be a good approximation for the μ-distortion amplitude. This window function and the analogous one for y distortions are shown in Fig. 1.

This simplified picture allows us to obtain a qualitative understanding of the possible constraints coming from an experiment like PIXIE [2].

We also account for adiabatic cooling [43,65], namely the fact that electrons and baryons alone would cool down faster than photons. Because of the continuous interactions, they effectively extract energy from the photons to maintain the same temperature, leading to an additional source of distortions of the CMB spectrum. During the μ era, this energy extraction results in a negative μ distortion of order

FIG. 1. This cartoon plot shows the scales which are probed by μ- and y-type spectral distortions, using the "window function" approximation of Eq. (5).

$\mu_{\mathrm{BEC}} \approx -2.7 \times 10^{-9}$ (for the Planck 2015 best-fit values of cosmological parameters).

III. EXPECTATIONS FROM LARGE SCALES

As we discussed in the previous section, the expected primordial spectral distortion μ is a function of cosmological parameters that play a role during the early Universe epoch (like the scalar spectral index n_s, its running α_s, the cold dark matter energy density, etc.). Since most of these parameters are now well constrained by the recent measurements of CMB anisotropies (both in temperature and polarization) made by the Planck satellite, one could, albeit indirectly, constrain the expected value of μ assuming a ΛCDM model or one of its extensions (see also Ref. [22] for a recent analysis).

Spectral distortions in the μ era can be computed in terms of six or seven parameters (which we will call $\boldsymbol{\theta}$):

(i) The baryon and cold dark matter density parameters $\Omega_b h^2 \equiv \omega_b$ and $\Omega_c h^2 \equiv \omega_c$, together with the number of effective relativistic degrees of freedom N_{eff}. These enter in the computation of the expansion history: from them we compute the Hubble constant H_0 and the helium mass fraction Y_P that enter in the computation of the dissipation scale k_D.

(ii) The CMB temperature T_{CMB}.

(iii) The parameters describing the primordial spectrum,

$$P_\zeta(k) = \frac{2\pi^2}{k^3} \Delta_\zeta(k) = A_s \left(\frac{k}{k_\star}\right)^{n_s - 1 + \frac{\alpha_s}{2}\log\frac{k}{k_\star}}, \quad (6)$$

namely the amplitude $\log(10^{10}A_s)$ and tilt n_s for the ΛCDM case, with the addition of the running α_s for the ΛCDM + α_s case.

We performed an analysis of the recent Planck TT, TE, EE + lowP likelihood [66], which includes the (temperature and E-mode polarization) high-ℓ likelihood together
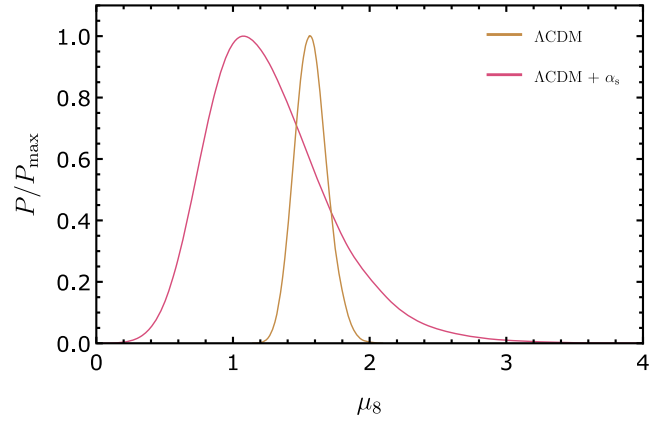

FIG. 2. The figure shows the one-dimensional posteriors for μ_8 predicted by Planck TT, TE, EE + lowP data, for the ΛCDM model (orange curve) and the ΛCDM + α_s model (purple curve). The posteriors have been obtained through the IDISTORT code developed by Khatri and Sunyaev [20,46].

with the TQU pixel-based low-ℓ likelihood, through Monte Carlo Markov chain sampling, using the publicly available code COSMOMC [67,68]. We have varied the primordial parameters, along with ω_b, ω_c, the reionization optical depth τ, and finally the ratio of the sound horizon to the angular diameter distance at decoupling $100\theta_{\mathrm{MC}}$. For each model in the MCMC chain we compute, as a derived parameter, the value of μ_8 using the IDISTORT code developed by Khatri and Sunyaev [20,46]. For this purpose we fix the CMB temperature to $T_{\mathrm{CMB}} = 2.7255$ K, the neutrino effective number to the standard value $N_{\mathrm{eff}} = 3.046$, and we evaluate the primordial helium abundance Y_P assuming standard big bang nucleosynthesis.

Processing the chains through the getdist routine (included in the COSMOMC package), and marginalizing over all the nuisance parameters, we obtain for the ΛCDM case (no running) the indirect constraint $\mu_8 = 1.57^{+0.108}_{-0.127}$ at 68% C.L. Including the possibility of a running, the Planck constraint on μ is weakened to $\mu_8 = 1.28^{+0.299}_{-0.524}$ (68% C.L.). The marginalized posterior distributions for μ_8 are shown in Fig. 2. Notice that the "the balanced injection scenario," namely the possibility that the negative contribution to μ from adiabatic cooling cancels precisely the positive contribution from the dissipation of adiabatic modes [63,65], leaving $\mu_8 = 0$, is excluded at extremely high significance (i.e. $\approx 15\sigma$) for the ΛCDM model, and at 97.4% C.L.[6] if we allow the running to vary.

Figure 3 shows the dependence of μ distortion on the tilt n_s and the running α_s.

(i) In the left panel we see that μ_8 is not very degenerate with n_s. The reason is twofold. First and most importantly, for nonzero running of order 10^{-2}, as

---

[6]We quote the confidence level, in this case, because the posterior for μ_8 is non-Gaussian (as can be seen from Fig. 2).
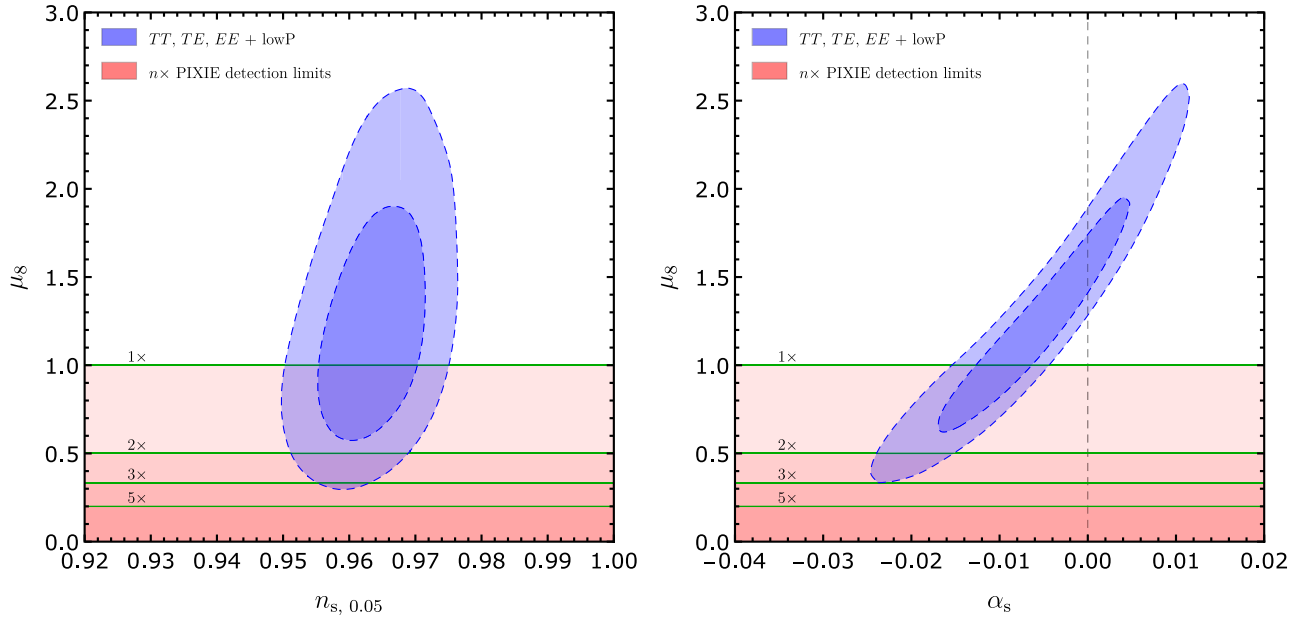
FIG. 3.   This figure shows the 68% C.L. and 95% C.L. contours in the n_s-μ (left panel) and the α_s-μ_8 plane (right panel) for the Planck TT, TE, EE + lowP data set for ΛCDM + α_s, together with the 1σ detection limits for PIXIE and possible improvements.

allowed by Planck, a change in the tilt of order 10^{-2} is a small correction to the power spectrum at the short scales that are responsible for μ distortions [α_s appears in Eq. (6) with a factor of $(\log k/k_\star)/2$–5 for $k \sim 10^3$ Mpc^{-1}]. Second, Planck constraints on n_s are tighter than those on α_s by roughly a factor of 2.

(ii) The right panel, on the other hand, shows that μ_8 is strongly dependent on α_s (increasing α_s increases the power at short scales and hence leads to a larger μ_8, and vice versa). We also note that the two dimensional-contour in the α_s-μ_8 plane is not ellipsoidal, but banana-shaped. The reason is that at large negative running, the contribution to spectral distortions from dissipation of acoustic waves will go to zero asymptotically, and the net μ amplitude will be the one from adiabatic cooling (which for the tightly constrained values of cosmological parameters can be practically considered a constant).

Having discussed the current (indirect) limits on μ distortions from Planck measurements of CMB temperature and polarization anisotropies, we move to the forecasts for a PIXIE-like spectrometer.

IV. FORECASTS FOR PIXIE: FISHER ANALYSIS

Considering only μ distortions, and using the approximation in terms of a window function from $z_1 = 5 \times 10^4$ to $z_2 = 2 \times 10^6$ (with the amplitude of the scalar spectrum fixed at $A_s \approx 2.2 \times 10^{-9}$), we can perform a simple Fisher forecast to see how the constraints on tilt and running are improved by combining PIXIE with the Planck prediction for μ_8.

This allows us also to discuss, mirroring what has been done for CMB anisotropies alone in Ref. [69], what is the optimal choice of pivot scale (that maximizes the detection power for these two parameters) for the combined analysis, as a function of the sensitivity of a PIXIE-like mission. We stress that the choice of pivot has no impact on the detectability of μ distortions themselves: it is just a particular way to parametrize the spectrum. Whether or not μ distortions will be seen is only dependent on the amount of scalar power at small scales (which is captured by the fiducial μ_8 that we consider).

Finally, we point out that an improvement of a factor of 3 over PIXIE implies a guaranteed discovery.

We add to the Planck bounds the detection limits for μ distortions from the PIXIE white paper [2], i.e.

$$\mathcal{L}(n_s, \alpha_s) \propto \mathcal{L}(n_s, \alpha_s)_{\text{Planck}}$$

$$\times \exp\left[-\frac{(\mu_8(n_s, \alpha_s) + \mu_{8,\text{BEC}} - \mu_8^{(\text{fid})})^2}{2\sigma_{\mu_8}^2}\right], \quad (7)$$

with $\sigma_{\mu_8} = 1$ (0.5 and 0.2) for ($2\times$ and $5\times$) PIXIE, and $\mu_8(n_s, \alpha_s)$ given by

TABLE I.   Mean and standard deviation for spectral index and running used in Eq. (9), from the Planck TT, TE, EE + lowP analysis.

$\bar{n}_s$	0.9639
$\bar{\alpha}_s$	−0.0057
σ_{n_s}	0.0050
σ_{α_s}	0.0071
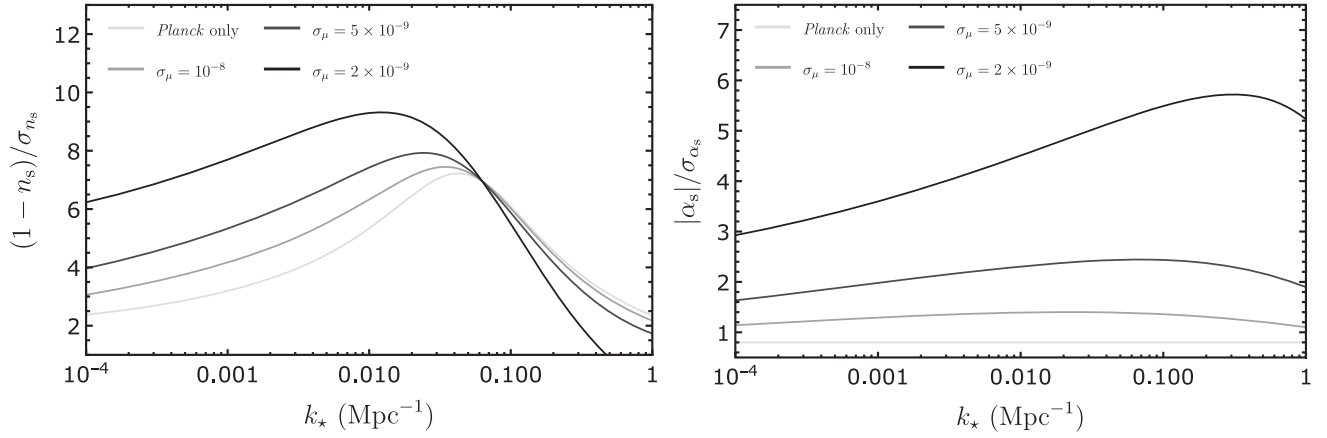
FIG. 4. $(1 - n_{\rm s})/\sigma_{n_{\rm s}}$ (left panel) and $|\alpha_{\rm s}|/\sigma_{\alpha_{\rm s}}$ (right panel) as a function of the pivot scale $k_\star$, for a vanishing fiducial distortions $\mu_8^{\rm (fid)} = 0$. A dependence on the pivot scale is always present for $n_{\rm s}$ (left panel), while for $\alpha_{\rm s}$ the dependence becomes appreciable only for significant improvements over PIXIE's sensitivity. The optimal choice of $k_\star$ shifts towards $k < 0.05$ Mpc^{-1} for $n_{\rm s}$ and $k > 0.05$ Mpc^{-1} for $\alpha_{\rm s}$, when the information from spectral distortions is included.
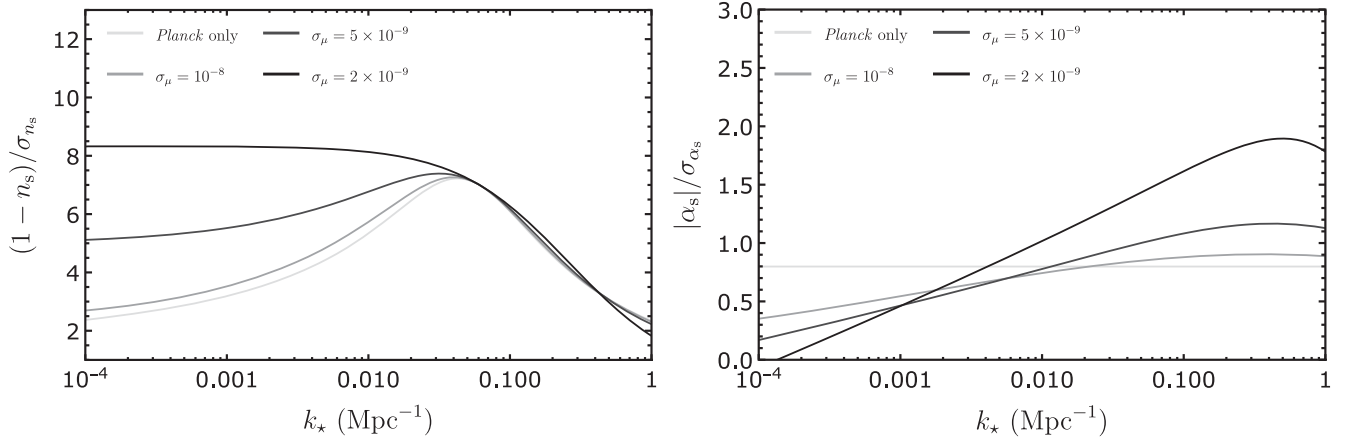

FIG. 5. Same as Fig. 4, but in this case we consider a fiducial μ_8 amplitude of 1.3 (see Sec. IV for details). The behavior is qualitatively similar to the case of a vanishing fiducial μ_8.

$$\mu_8(n_{\rm s}, \alpha_{\rm s}) = 2.3 \times 10^8$$
$$\times A_{\rm s} \int_{k_{\rm D}(z_1)}^{k_{\rm D}(z_2)} \frac{{\rm d}k}{k} \left(\frac{k}{k_\star}\right)^{n_{\rm s} - 1 + \frac{\alpha_{\rm s}}{2}\log\frac{k}{k_\star}}. \qquad (8)$$

The results of this Fisher analysis are just an approximation of the full MCMC sampling of the joint likelihood that we will present in the next section. We can then safely consider only two fiducial values for μ_8, which approximate well the choices we will make later (see Table II):

(i) $\mu_8^{\rm (fid)} = 0$, i.e. a cosmology with zero μ-type distortions;

(ii) $\mu_8^{\rm (fid)} = 1.3$, i.e. the mean-fit value from Planck data (for the ΛCDM + $\alpha_{\rm s}$ case).

For the Planck likelihood, we take (disregarding for simplicity the normalization)

$$\log \mathcal{L}(n_{\rm s}, \alpha_{\rm s})_{\rm Planck} = -\frac{(\alpha_{\rm s} - \bar{\alpha}_{\rm s})^2}{2\sigma_{\alpha_{\rm s}}^2}$$
$$- \frac{(n_{\rm s} + \frac{\alpha_{\rm s}}{2}\log(k_\star/k_\star^{(0)}) - \bar{n}_{\rm s})^2}{2\sigma_{n_{\rm s}}^2}, \qquad (9)$$

where

(i) the tilt is written at an arbitrary pivot $k_\star$ in terms of the running and the reference scale $k_\star^{(0)}$ (note that the Jacobian of the transformation is 1 so it can be neglected);

(ii) $k_\star^{(0)} = 0.05$ Mpc^{-1} is the scale where $n_{\rm s}$ and $\alpha_{\rm s}$ decorrelate: for this reason we take $\bar{n}_{\rm s}, \bar{\alpha}_{\rm s}$ to be the marginalized means from the Planck TT, TE, EE + lowP analysis. $\sigma_{n_{\rm s}}$ and $\sigma_{\alpha_{\rm s}}$ are the corresponding marginalized standard deviations. The values are listed in Table I.

TABLE II. 68% C.L. constraints on the scalar spectral index n_s, its running α_s and the μ-distortion amplitude from a future combined analysis of the Planck 2015 release in temperature and polarization and a PIXIE-like spectrometer as a function of different experimental configurations and fiducial values for μ_8. Notice that for $\alpha_s^{(\mathrm{fid})} = -0.01$, $5 \times$ PIXIE is needed to exclude $\alpha_s = 0$ at 95% C.L., while for $\alpha_s^{(\mathrm{fid})} = -0.02$, $3 \times$ PIXIE suffices.

TT, TE, EE + lowP	n_s	α_s	μ_8
ΛCDM	$0.9645^{+0.0048}_{-0.0049}$	$\equiv 0$	$1.57^{+0.11}_{-0.13}$
ΛCDM + α_s	0.9639 ± 0.0050	$-0.0057^{+0.0071}_{-0.0070}$	$1.28^{+0.30}_{-0.52}$
"slow-roll"	$0.9644^{+0.0051}_{-0.0052}$	$\sim -(1 - n_s)^2$	$1.49^{+0.12}_{-0.13}$
$\alpha_s^{(\mathrm{fid})} = -0.01$ ($\mu_8^{(\mathrm{fid})} = 1.06$)	n_s	α_s	μ_8
Planck + $1 \times$ PIXIE	$0.9637^{+0.0050}_{-0.0049}$	$-0.0064^{+0.0065}_{-0.0064}$	$1.22^{+0.28}_{-0.45}$
Planck + $2 \times$ PIXIE	$0.9634^{+0.0049}_{-0.0048}$	$-0.0074^{+0.0061}_{-0.0053}$	$1.15^{+0.25}_{-0.34}$
Planck + $3 \times$ PIXIE	0.9632 ± 0.0048	$-0.0079^{+0.0053}_{-0.0045}$	$1.11^{+0.22}_{-0.27}$
Planck + $5 \times$ PIXIE	$0.9631^{+0.0048}_{-0.0047}$	$-0.0083^{+0.0040}_{-0.0035}$	$1.08^{+0.17}_{-0.18}$
Planck + $10 \times$ PIXIE	0.9631 ± 0.0047	$-0.0085^{+0.0025}_{-0.0024}$	1.06 ± 0.09
$\alpha_s^{(\mathrm{fid})} = -0.02$ ($\mu_8^{(\mathrm{fid})} = 0.73$)	n_s	α_s	μ_8
Planck + $1 \times$ PIXIE	$0.9635^{+0.0050}_{-0.0049}$	$-0.0071^{+0.0065}_{-0.0063}$	$1.18^{+0.27}_{-0.43}$
Planck + $2 \times$ PIXIE	$0.9628^{+0.0049}_{-0.0048}$	$-0.0094^{+0.0061}_{-0.0052}$	$1.04^{+0.23}_{-0.31}$
Planck + $3 \times$ PIXIE	$0.9624^{+0.0049}_{-0.0048}$	$-0.0111^{+0.0055}_{-0.0045}$	$0.95^{+0.19}_{-0.24}$
Planck + $5 \times$ PIXIE	$0.9618^{+0.0049}_{-0.0047}$	$-0.0131^{+0.0046}_{-0.0037}$	$0.85^{+0.16}_{-0.15}$
Planck + $10 \times$ PIXIE	$0.9613^{+0.0048}_{-0.0047}$	$-0.0149^{+0.0033}_{-0.0029}$	0.77 ± 0.09

Figure 4 shows $(1 - n_s)/\sigma_{n_s}$ and $|\alpha_s|/\sigma_{\alpha_s}$ as a function of the pivot scale for vanishing $\mu^{(\mathrm{fid})}$: we see that, as we increase the sensitivity of PIXIE, the $k_\star$ that maximizes the detection of the tilt is shifted towards values smaller than $k_\star^{(0)} = 0.05 \ \mathrm{Mpc}^{-1}$. The best pivot for the running moves in the opposite direction, towards values larger than $0.05 \ \mathrm{Mpc}^{-1}$. Figure 5 shows that the same qualitative behavior is reproduced in the case of a fiducial μ_8 different from zero.

These plots show that the effect of changing the pivot on the detection power for n_s and α_s is not very relevant, if we increase $1/\sigma_{\mu_8}$ up to $5 \times$ PIXIE. At $10\times$ the choice of $k_\star$ can lead to a small improvement on σ_{α_s}: this is an interesting result, that could open up the possibility of choosing the pivot outside of the CMB window in the future, as σ_{μ_8} becomes even smaller.[7] However, since we will stop at $10 \times$ PIXIE (i.e. the expected error on μ_8 achievable by PRISM) in this work, we will keep $k_\star = 0.05 \ \mathrm{Mpc}^{-1}$ in the following sections.

For vanishing $\mu_8^{(\mathrm{fid})}$, Fig. 4 shows that the improvement for σ_{α_s} can be greater than the case with nonzero fiducial. However, it is important to stress that the assumption of having zero distortions starts to become incompatible with the Planck indirect constraints on μ_8 (as one can see, e.g.,

from Fig. 2) for $\sigma_{\mu_8} \approx 0.3$, making a combination of the two likelihoods inadvisable (this is also the reason why we have decided to not consider, in Sec. I, a fiducial running so small that spectral distortions from Silk damping are absent). For fiducial μ_8 different from zero we see that this does not happen: the combination of the likelihoods, which we will explore through MCMC sampling in the next section, is therefore justified in this case.

Finally, it is interesting to ask whether there exists any threshold value for sensitivity to the μ amplitude such that, by reaching it, we are guaranteed to learn something about the early Universe, irrespective of what the running might actually be. The right panel of Fig. 4 suggests the answer to this question (which we will confirm in the next section with a detailed calculation). Within the uncertainty of Planck, a vanishing running implies a distortion of order $\mu_8 \sim 1.4$, as we have seen in Sec. III: therefore a measurement of the CMB spectrum at a sensitivity of $\sigma_{\mu_8} \sim 1.4/4 = 0.35$, corresponding to about $3 \times$ PIXIE, must lead to[8] a first detection of μ distortions or a detection of negative running, or both. In fact, any central value $\mu_8 \lesssim 1.4/2 \sim 0.7$ at this resolution would exclude $\alpha_s \geq 0$, while any larger μ_8 would exclude $\mu_8 \leq 0$ at 95% C.L.

---

[7]However, from the left panels of Figs. 4 and 5 we see how this improvement would be at the expense of an increased error on the tilt n_s.

[8]This assumes that we interpret the data within ΛCDM plus running. Given our theoretical understanding of the early Universe, this is indeed perhaps the most natural choice.

V. FORECASTS FOR PIXIE: MCMC

This section contains the main results of the paper, summarized in Table II and Fig. 6 (which shows the contours in the α_s-μ_8 plane).

We start with a discussion of the detectability of μ-type distortions by PIXIE in the context of the ΛCDM model, i.e. with zero running of the spectral index. We stress that, in this case, Planck bounds imply that with only a small $2\times$ improvement over PIXIE's noise, the exclusion of $\mu_8 \leq 0$ at $\approx 3\sigma$ is guaranteed, given the narrow posterior for μ_8.

On the other hand, as we have seen in Sec. III, for the ΛCDM $+ \alpha_s$ case a value of $\mu_8 \sim 0.7$ is fully compatible with Planck data, and it will be only marginally detectable by PIXIE in the case of a minimal configuration. Assuming the Planck constraint on μ_8, the minimal value of μ_8 compatible with Planck in between two standard deviations is $\mu_8 \sim 0.25$. Clearly, given this value, a safe experimental direct detection of μ-type distortions can be obtained only with an experimental sensitivity of $\sigma_{\mu_8} \sim 0.2$, i.e. a $5\times$ improvement over PIXIE.

However, in the presence of running, the argument can be reversed: now it becomes interesting to see how precise the measurement performed by a PIXIE-like spectrometer should be in order to translate a nondetection of μ distortions into a detection of $\alpha_s < 0$, pursuing the marginal (below one standard deviation) indication for negative running coming from Planck (whose posterior, while compatible with $\alpha_s = 0$, peaks at a negative value of $\alpha_s = -0.006$; see Table II). For this purpose, we reprocess

the MCMC chains by importance sampling, multiplying the weight of each sample by [see also Eq. (7)]

$$\mathcal{L}_{\text{PIXIE}} = \exp\left[-\frac{(\mu_8(\boldsymbol{\theta}) + \mu_{8,\text{BEC}}(\boldsymbol{\theta}) - \mu_8^{(\text{fid})})^2}{2\sigma_{\mu_8}^2}\right], \quad (10)$$

focussing on the two fiducial models for the running described in Sec. I:

(i) $\alpha_s^{(\text{fid})} = -0.01$, corresponding to a spectral distortion $\mu_8 = 1.06$ (close to the Planck best fit for μ_8);

(ii) $\alpha_s^{(\text{fid})} = -0.02$ corresponding to a spectral distortion $\mu_8 = 0.73$, which is at the limit of two standard deviations from the Planck mean fit.

As in Sec. IV, we take $\sigma_{\mu_8} = 1/n$ for a $n \times$ PIXIE experimental configuration. The results of this importance sampling are also reported in Table II.

Considering that from the Planck data set alone one obtains $\sigma_{n_s} \approx 0.005$ and $\sigma_{\alpha_s} \approx 0.007$, we see that the minimal configuration of $1 \times$ PIXIE or the upgraded $2 \times$ PIXIE will produce minimal effects on the Planck bounds, even when the fiducial model deviates significantly from the Planck best fit.

If, instead, the experimental sensitivity will reach the level of $5 \times$ PIXIE ($10 \times$ PIXIE) then the constraints on the running of the spectral index can be improved by $\sim 30\%$ ($\sim 50\%$): this improvement could be extremely significant. More precisely, we see that if $\alpha_s^{(\text{fid})}$ is ~ -0.01, then the addition of $5 \times$ PIXIE to Planck bounds could yield a detection of negative running at two standard deviations
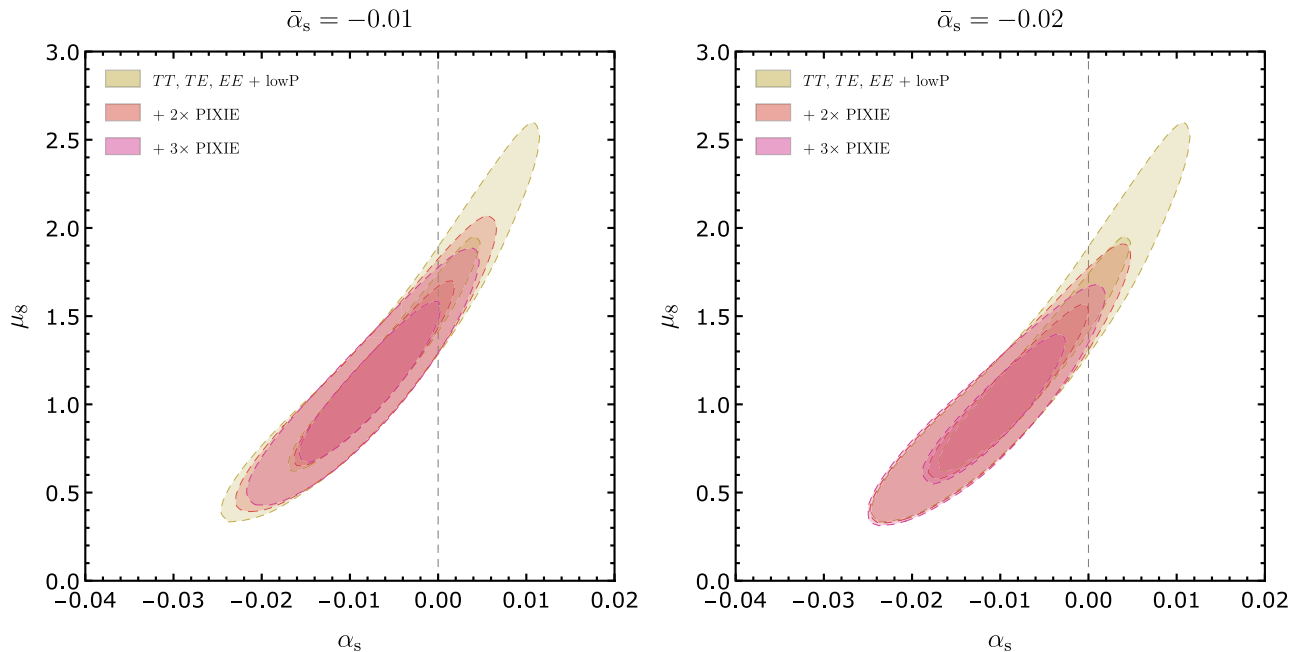

FIG. 6. Left panel: 68% C.L. and 95% C.L. contours in the α_s-μ_8 plane, for Planck alone (yellow contour) and including in the analysis the likelihood with $\alpha_s^{(\text{fid})} = -0.01$ (i.e. $\mu_8^{(\text{fid})} = 1.06$) for a $2\times$ and $3\times$ improvement over PIXIE (orange and purple contours). Right panel: Same as left panel, but with the fiducial α_s equal to -0.02.

(three for $10 \times$ PIXIE). If we allow an even more negative fiducial value for the running, i.e. $\alpha_s^{(fid)} \sim -0.02$ then the negative running will be probed at two standard deviations by $3 \times$ PIXIE (five standard deviations by $10 \times$ PIXIE). Table II also shows that the constraints on the tilt are left basically untouched, in agreement with the results of Sec. III, where we have seen that μ_8 is only mildly dependent on it.

Finally, we comment on the possibility of discriminating between no-running ΛCDM and slow-roll inflation, where the running is second order in the slow-roll expansion. An order-of-magnitude prediction for α_s, that arises in many models, is $\alpha_s \sim -(1 - n_s)^2$ [23–25]: Table II shows that the predictions for μ_8 in these two cases are indistinguishable at PIXIE's sensitivity, and that a massive improvement in sensitivity by a factor of order 10^2 is needed to probe the differences between them.

VI. IMPLICATIONS FOR SLOW-ROLL INFLATION

In this section, we discuss the implications of the value of the running within single-clock inflation. Observations tell us (see Ref. [1] and Table II)

$$1 - n_s(k_\star) \equiv -\frac{\partial \log \Delta_\zeta^2(k_\star)}{\partial \log k} \tag{11}$$

$$= 0.0361 \pm 0.0050 \quad (68\% \text{ C.L.}),$$

$$\alpha_s = -n_{s,N} \tag{12}$$

$$= -0.0057^{+0.0071}_{-0.0070} \quad (68\% \text{ C.L.}),$$

$$r < 0.08 \quad (95\% \text{ C.L.}), \tag{13}$$

where $*_{,N}$ refers to a derivative with respect to the number of e-foldings from the end of inflation, decreasing as time increases, namely $Hdt = -dN$ (we refer to Ref. [70] for a comprehensive review). The standard slow-roll solution for the primordial power spectrum gives (for an inflaton speed of sound c_s)

$$1 - n_s = 2\epsilon - \frac{\epsilon_{,N}}{\epsilon} - \frac{c_{s,N}}{c_s} \tag{14}$$

$$= \frac{r}{8c_s} - \frac{r_{,N}}{r}, \tag{15}$$

$$\alpha_s = 2\epsilon_{,N} - \frac{r_{,NN}}{r} + \left(\frac{r_{,N}}{r}\right)^2, \tag{16}$$

where the tensor-to-scalar ratio is given approximately by $r = 16\epsilon c_s$.

It is convenient to reexpress the running by making explicit its dependence on the tilt, which is relatively well constrained, i.e.
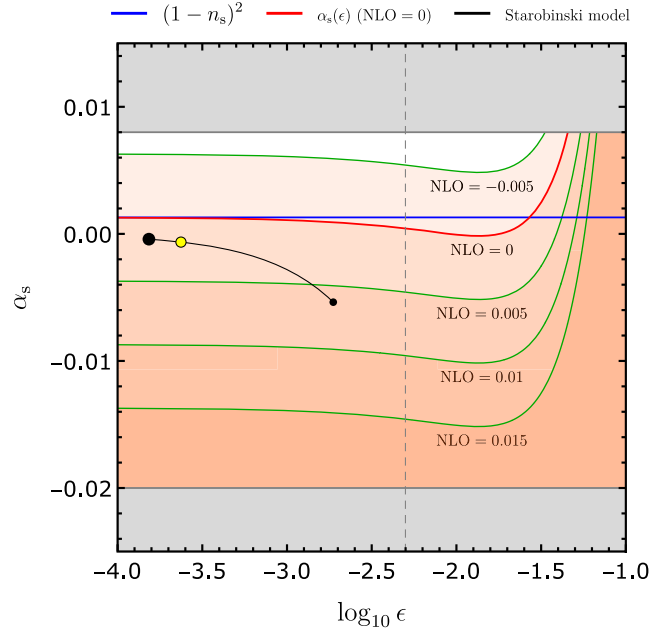

FIG. 7. This contour plot shows α_s as a function of ϵ for different values of the NLO slow-roll parameters. Notice that the uncertainty in n_s is smaller than the thickness of the lines in the plot. In red we show $\alpha(\epsilon)$ of Eq. (17) for NLO $= 0$, while the blue line is its asymptotic value $(1 - n_s)^2 \approx 0.0013$. The black line shows the predictions of the Starobinsky model [71] (with N going from 20 to 70), with the yellow dot being its prediction for $N = 56$ (chosen to reproduce the observed value of n_s). The gray bands show the values of α_s excluded (at 95% C.L.) by Planck TT, TE, EE + lowP data, while the gray dashed vertical line shows the current bound on $\epsilon = r/(16c_s)$ from Eq. (13), considering $c_s = 1$.

$$\alpha_s = (1 - n_s)^2 - 6\epsilon(1 - n_s) + 8\epsilon^2 - \left(\frac{rs}{8c_s} + \frac{r_{,NN}}{r}\right). \tag{17}$$

Here, ϵ can be extracted from r if we know the speed of sound c_s from the equilateral bispectrum, or if we assume standard slow-roll single-field inflation, namely $c_s = 1$. On the other hand, the last term $r_{,NN}/r$ makes its first appearance in the running α_s; also the penultimate term $s \equiv c_{s,N}/c_s$ is degenerate with $\epsilon_{,N}/\epsilon$ in n_s and so it is also considered unknown. In this precise sense, we can think of the running as a measurement of the yet unknown next-to-leading-order (NLO) slow-roll parameters

$$\text{NLO} \equiv \frac{rs}{8c_s} + \frac{r_{,NN}}{r} \stackrel{c_s=1}{\to} \frac{\epsilon_{,NN}}{\epsilon}. \tag{18}$$

In Fig. 7, we show a contour plot of α_s as a function of ϵ for different values of the NLO slow-roll parameters. We point out that for NLO $= 0$ one finds $\alpha \geq -\frac{1}{8}(1 - n_s)^2 \simeq -2 \times 10^{-4}$. Any evidence that the running is sizable and negative therefore implies NLO > 0, i.e. the discovery of a new higher-order slow-roll parameter. In a

typical slow-roll model, one indeed expects the NLO terms to be of the same order as $(1 - n_s)^2$. For example, consider $c_s = 1$ and $\epsilon = 3/(4N^2)$,[9] i.e. the Starobinsky model [71]. Then we have

$$(1 - n_s)^2 \simeq \frac{4}{N^2}, \tag{19}$$

$$\frac{r_{,NN}}{r} = \frac{6}{N^2}. \tag{20}$$

One hence finds

$$\alpha_s \simeq -\frac{2}{N^2} \simeq -\frac{1}{2}(1 - n_s)^2. \tag{21}$$

VII. CONCLUSION

In this work, we have considered how a measurement of the CMB spectrum by an experiment like PIXIE would extend our knowledge of the very early Universe. Using Planck data, we have derived the predicted likelihood for the size of the μ-type distortions generated by the dissipation of acoustic waves in the photon-baryon-electron plasma. As shown in Fig. 2, both ΛCDM and ΛCDM $+ \alpha_s$ predict $\mu_8 \simeq \mathcal{O}(1)$, and exclude $\mu_8 = 0$, a.k.a. the "the balanced injection scenario" [43,63,65] at high confidence (at 15σ for ΛCDM, and at 97.4% C.L. for ΛCDM $+ \alpha_s$). While this means that we will eventually be able to measure μ distortions, it is important to determine whether this will already be possible with the next satellite experiment. Here we point out that, irrespective of the actual value of α_s [and its respective μ_8, according to Eq. (8)], a meaningful sensitivity target is $\sigma_{\mu_8} \simeq 0.35$, namely about a 3$\times$ improvement over the current PIXIE design (but still less sensitive than the proposed PRISM). This is in fact the threshold for a guaranteed discovery: either μ_8 is large enough that it will be detected (at 95% C.L.), or else $\alpha_s \geq 0$ will be excluded (at 95% C.L.) and with it our current standard model, namely the six-parameter ΛCDM. The absence of a detection of μ_8 for a $3 \times$ PIXIE improvement would exclude most slow-roll models as well, since typically $|\alpha_s| \sim (1 - n_s)^2$, which is indistinguishable from $\alpha_s = 0$ at these sensitivities.

We have further considered the constraining power of CMB spectral distortions combined with the current Planck data. We have discussed how to optimize this analysis by choosing an appropriate pivot for the parametrization of the primordial power spectrum (see Fig. 4 and Fig. 5). In Table II, we present the improved constraints on the spectral tilt and its running from Planck plus an n-fold

---

[9]Note that the relation $\epsilon = 3/(4N^2)$ holds at first order in slow roll: it is accurate enough, however, for the values of N that reproduce a scalar spectral index n_s within the current Planck bounds.

improvement over PIXIE sensitivity. For a fiducial $\alpha_s = -0.01$, close to the fit for Planck, one expects a detection of μ_8 at 95% C.L. already with $2 \times$ PIXIE. Conversely, for a fiducial $\alpha_s = -0.02$ (which is at the low 95% C.L. end of the Planck constraint), $3 \times$ PIXIE will already provide evidence (at 2σ) of a sizable negative running. This would put pressure on the standard slow-roll paradigm, which leads to the typical expectation $\alpha_s \simeq (1 - n_s)^2$ [see, e.g., Eq. (17)]. Finally, we proposed Fig. 7 as a convenient and compact way to visualize the improving constraints on the tilt, running and tensor-to-scalar ratio.

APPENDIX A: μ DISTORTION FROM ENERGY RELEASE $E \to E + \delta E$

The relation $\mu \approx 1.4 \times \delta E/E$ can be understood with the following simple calculation, recalling that during the μ era the total number of photons is conserved. Taking a Bose-Einstein spectrum with energy $E + \delta E$ and small chemical potential μ, and expressing the temperature T in terms of energy and chemical potential as

$$T = \frac{\sqrt[4]{15}\sqrt[4]{E}}{\sqrt{\pi}}\left(1 + \frac{1}{4}\frac{\delta E}{E} + \frac{45\zeta(3)}{2\pi^4}\mu\right) + \mathcal{O}^2, \tag{A1}$$

one can find the relation between δE and μ by requiring that the increase of energy is not accompanied by an increase in the number of photons, which remains equal to that of the original Planck spectrum, i.e.

$$N_{\text{B-E}}(T(E + \delta E, \mu), \mu) = N_{\text{Planck}}(E). \tag{A2}$$

Solving for μ, one finds [11,72]

$$\mu = \frac{9\pi^4\zeta(3)}{2(\pi^6 - 405\zeta(3)^2)}\frac{\delta E}{E} \approx 1.4 \times \frac{\delta E}{E}. \qquad \text{(A3)}$$

APPENDIX B: SPECTRAL SHAPES AND S/N FOR PIXIE

If we consider Eq. (2), we see that we can write down the observed photon spectrum in terms of shapes $\mathcal{I}_a$ and corresponding amplitudes μ_a where, for example [11,72]

   (i) $a = 1$ corresponds to a μ-type occupation number, i.e. (recalling that $x \equiv h\nu/k_{\rm B}T$)

$$\mathcal{I}_1 = \frac{2h\nu^3}{c^2}\frac{e^x}{(e^x - 1)^2}\left(\frac{x}{2.19} - 1\right)$$
$$\equiv \frac{2h\nu^3}{c^2} \times n^{(\mu)}(\nu), \qquad \text{(B1)}$$

   (ii) $a = 2$ corresponds to a y-type occupation number, i.e.

$$\mathcal{I}_2 = \frac{2h\nu^3}{c^2}\frac{xe^x}{(e^x - 1)^2}\left[x\left(\frac{e^x + 1}{e^x - 1}\right) - 4\right]$$
$$\equiv \frac{2h\nu^3}{c^2} \times n^{(y)}(\nu) \qquad \text{(B2)}$$

and so on. Besides μ-, i- and y-type distortions, that we have discussed in Sec. II, one must also consider the fact that the uniform part of temperature perturbations Θ is not known *a priori* and must be fit simultaneously with the spectral distortions: for this reason we also consider the t-type occupation number, i.e. [20]

$$\mathcal{I}_t = \frac{2h\nu^3}{c^2}\frac{xe^x}{(e^x - 1)^2}$$
$$\equiv \frac{2h\nu^3}{c^2} \times n^{(t)}(\nu). \qquad \text{(B3)}$$

We do not include foregrounds in our analysis since, for PIXIE, the noise penalty for rejecting foregrounds is only 2%, and this noise penalty has been included in all the estimates of CMB sensitivity by the PIXIE Collaboration [2].

We can then write down the signal-to-noise, in terms of amplitudes μ_a and spectra $\mathcal{I}_a$ as (dropping factors of 2 for simplicity)

$$\left(\frac{S}{N}\right)^2 = \sum_c \frac{[\sum_a \mathcal{I}_a(\nu_c) \times (\mu_a - \bar\mu_a)]^2}{(\delta I(\nu_c))^2}, \qquad \text{(B4)}$$

where $\bar\mu_a$ are the fiducial values of the amplitudes, and $\delta I(\nu_c)$ is the noise at each frequency channel c.
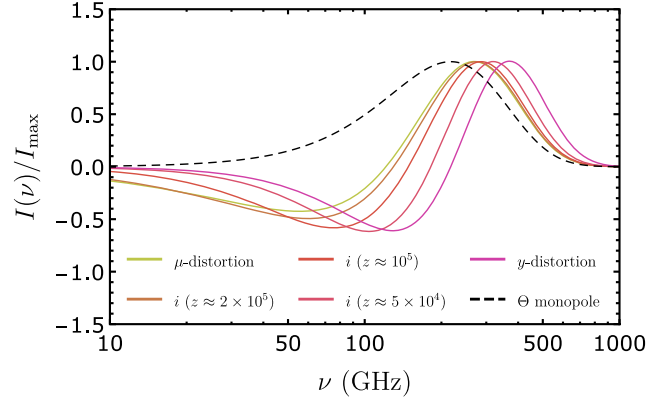

FIG. 8. This plot shows the spectral shapes (normalized at the maximum) $I(\nu)$ for μ and y distortions, together with the spectra for i-type distortions at redshifts $z = \mathcal{O}(2 \times 10^5)$, $z = \mathcal{O}(1 \times 10^5)$ and $z = \mathcal{O}(5 \times 10^4)$ and the spectral shape of the monopole of temperature anisotropies Θ. We see that for increasing redshift, the maximum, minimum and zero of the occupation numbers are moved towards lower frequencies.

   (i) PIXIE will have 400 channels (15 GHz wide) from 30 GHz to 6 THz; however, we see from Fig. 8 that the signals that we consider go quickly to zero beyond $\nu \approx 1000$, so the sum over channels in Eq. (B4) will stop there.

   (ii) δI for PIXIE, as from Fig. 12 of Ref. [2], is expected to be 5×10^{-26} W m^{-2} Hz^{-1} sr^{-1}.

If we want to marginalize over some of the amplitudes μ_a (see Ref. [73], for example), we can use the fact that for a Gaussian with inverse covariance matrix (Fisher matrix) F given by

$$F = \begin{pmatrix} \tilde{F} & S \\ S^T & M \end{pmatrix}, \qquad \text{(B5)}$$

where $\tilde{F}$ is the submatrix that spans the parameters that we are interested in, the marginalized Fisher matrix will be equal to

$$F_{\rm marg} = \tilde{F} - SM^{-1}S^T. \qquad \text{(B6)}$$

For Eq. (B4), we will want to marginalize over t and y, so M will be the 2×2 matrix

$$M_{ab} = \sum_c \frac{\mathcal{I}_a(\nu_c)\mathcal{I}_b(\nu_c)}{\delta I(\nu_c)\,\delta I(\nu_c)}, \qquad \text{(B7)}$$

with $a, b = y, t$. Similar expressions can be derived for S and its transpose, while $\tilde{F}$ is simply given by Eq. (B4) with a running on all components except y and t. If we had instead supposed that the two y and t amplitudes were known, we could just have taken $\tilde{F}$ as the Fisher matrix for Eq. (B4).

In this work we have not considered i distortions, so F will be a 3×3 matrix with $a, b, c = \mu, y, t$: marginalizing over y and t amplitudes, as described in Eqs. (B6) and (B7), we obtain $\sigma_{\mu_8} = 1$ for the standard PIXIE configuration. The increments in PIXIE sensitivity that we considered in the text, then, can be interpreted as either an increase in the number N of frequency channels (that would decrease σ_{μ_8} by a factor $\sqrt{N^{PIXIE}/N^{new}}$), or a decrease in the instrumental noise δI (which instead gives a linear improvement $\delta I^{new}/\delta I^{PIXIE}$).

[1] P. A. R. Ade *et al.* (Planck Collaboration), arXiv: 1502.02114.

[2] A. Kogut *et al.*, J. Cosmol. Astropart. Phys. 07 (2011) 025.

[3] P. André *et al.* (PRISM Collaboration), arXiv:1306.2259.

[4] P. André *et al.* (PRISM Collaboration), J. Cosmol. Astropart. Phys. 02 (2014) 006.

[5] F. R. Bouchet *et al.* (COrE Collaboration), arXiv: 1102.2181.

[6] T. Matsumura *et al.*, J. Low Temp. Phys. **176**, 733 (2014).

[7] M. Zaldarriaga and U. Seljak, Phys. Rev. D **55**, 1830 (1997).

[8] M. Kamionkowski, A. Kosowsky, and A. Stebbins, Phys. Rev. D **55**, 7368 (1997).

[9] P. Creminelli, D. L. López Nacir, M. Simonović, G. Trevisan, and M. Zaldarriaga, J. Cosmol. Astropart. Phys. 11 (2015) 031.

[10] G. Cabass, L. Pagano, L. Salvati, M. Gerbino, E. Giusarma, and A. Melchiorri, Phys. Rev. D **93**, 063508 (2016).

[11] R. A. Sunyaev and Y. B. Zeldovich, Astrophys. Space Sci. **7**, 20 (1970).

[12] W. Hu and J. Silk, Phys. Rev. D **48**, 485 (1993).

[13] E. Dimastrogiovanni, L. M. Krauss, and J. Chluba, arXiv: 1512.09212.

[14] M. Anthonisen, R. Brandenberger, A. Laguë, I. A. Morrison, and D. Xia, J. Cosmol. Astropart. Phys. 02 (2016) 047.

[15] J. M. Wagstaff and R. Banerjee, Phys. Rev. D **92**, 123004 (2015).

[16] K. E. Kunze and M. Á. Vázquez-Mozo, J. Cosmol. Astropart. Phys. 12 (2015) 028.

[17] Y. Ali-Haïmoud, J. Chluba, and M. Kamionkowski, Phys. Rev. Lett. **115**, 071304 (2015).

[18] J. B. Dent, D. A. Easson, and H. Tashiro, Phys. Rev. D **86**, 023514 (2012).

[19] J. Chluba, A. L. Erickcek, and I. Ben-Dayan, Astrophys. J. **758**, 76 (2012).

[20] R. Khatri and R. A. Sunyaev, J. Cosmol. Astropart. Phys. 06 (2013) 026.

[21] S. Clesse, B. Garbrecht, and Y. Zhu, J. Cosmol. Astropart. Phys. 10 (2014) 046.

[22] K. Enqvist, T. Sekiguchi, and T. Takahashi, arXiv: 1511.09304.

[23] D. Roest, J. Cosmol. Astropart. Phys. 01 (2014) 007.

[24] J. Garcia-Bellido and D. Roest, Phys. Rev. D **89**, 103527 (2014).

[25] R. Gobbetti, E. Pajer, and D. Roest, J. Cosmol. Astropart. Phys. 09 (2015) 058.

[26] P. A. R. Ade *et al.* (Planck Collaboration), arXiv:1502. 01589.

[27] J. Silk, Astrophys. J. **151**, 459 (1968).

[28] P. J. E. Peebles and J. T. Yu, Astrophys. J. **162**, 815 (1970).

[29] N. Kaiser, Mon. Not. R. Astron. Soc. **202**, 1169 (1983).

[30] S. Galli, K. Benabed, F. Bouchet, J.-F. Cardoso, F. Elsner, E. Hivon, A. Mangilli, S. Prunet, and B. Wandelt, Phys. Rev. D **90**, 063504 (2014).

[31] W. L. K. Wu, J. Errard, C. Dvorkin, C. L. Kuo, A. T. Lee, P. McDonald, A. Slosar, and O. Zahn, Astrophys. J. **788**, 138 (2014).

[32] O. Doré *et al.*, arXiv:1412.4872.

[33] J. Errard, S. M. Feeney, H. V. Peiris, and A. H. Jaffe, J. Cosmol. Astropart. Phys. 03 (2016) 052.

[34] E. Pajer and M. Zaldarriaga, Phys. Rev. Lett. **109**, 021302 (2012).

[35] N. Arkani-Hamed, H. C. Cheng, P. Creminelli, and L. Randall, Phys. Rev. Lett. **90**, 221302 (2003).

[36] B. Feng, M. z. Li, R. J. Zhang, and X. m. Zhang, Phys. Rev. D **68**, 103511 (2003).

[37] T. Kobayashi and F. Takahashi, J. Cosmol. Astropart. Phys. 01 (2011) 026.

[38] R. K. Jain, M. Sandora, and M. S. Sloth, J. Cosmol. Astropart. Phys. 06 (2015) 016.

[39] S. Parameswaran, G. Tasinato, and I. Zavala, arXiv: 1602.02812.

[40] A. F. Illarionov and R. A. Sunyaev, Sov. Astron. **18**, 691 (1975).

[41] L. Danese and G. De Zotti, Astropart. Phys. **107**, 39 (1982).

[42] L. Danese and G. De Zotti, Astron. Astrophys. **246**, 49 (1991).

[43] J. Chluba and R. A. Sunyaev, Mon. Not. R. Astron. Soc. **419**, 1294 (2012).

[44] R. Khatri and R. A. Sunyaev, J. Cosmol. Astropart. Phys. 06 (2012) 038.

[45] R. A. Sunyaev and R. Khatri, Int. J. Mod. Phys. D **22**, 1330014 (2013).

[46] R. Khatri and R. A. Sunyaev, J. Cosmol. Astropart. Phys. 09 (2012) 016.

[47] A. S. Kompaneets, Zh. Eksp. Teor. Fiz. **31**, 876 (1957) [Sov. Phys. JETP **4**, 730 (1957)].

[48] J. Chluba, Mon. Not. R. Astron. Soc. **434**, 352 (2013).

[49] J. Chluba, Mon. Not. R. Astron. Soc. **436**, 2232 (2013).

[50] J. C. Hill and E. Pajer, Phys. Rev. D **88**, 063526 (2013).

[51] J. C. Hill, N. Battaglia, J. Chluba, S. Ferraro, E. Schaan, and D. N. Spergel, Phys. Rev. Lett. **115**, 261301 (2015).

[52] J. C. Hill, arXiv:1510.06237.

[53] J. Chluba and D. Jeong, Mon. Not. R. Astron. Soc. **438**, 2065 (2014).

[54] J. Chluba and Y. Ali-Haimoud, Mon. Not. R. Astron. Soc. **456**, 3494 (2016).

[55] K. Basu, C. Hernandez-Monteagudo, and R. Sunyaev, Astron. Astrophys. **416**, 447 (2004).

[56] G. De Zotti, M. Negrello, G. Castex, A. Lapi, and M. Bonato, J. Cosmol. Astropart. Phys. 03 (2016) 047.

[57] P. J. E. Peebles, Astrophys. J. **153**, 1 (1968).

[58] Y. B. Zeldovich, V. G. Kurt, and R. A. Sunyaev, Zh. Eksp. Teor. Fiz. **55**, 278 (1968) [J. Exp. Theor. Phys. **28**, 146 (1969)].

[59] V. K. Dubrovich, Sov. Astron. Lett. **1**, 196 (1975).

[60] J. Chluba and R. A. Sunyaev, Astron. Astrophys. **446**, 39 (2006).

[61] J. A. Rubino-Martin, J. Chluba, and R. A. Sunyaev, Mon. Not. R. Astron. Soc. **371**, 1939 (2006).

[62] J. Chluba, J. A. Rubino-Martin, and R. A. Sunyaev, Mon. Not. R. Astron. Soc. **374**, 1310 (2007).

[63] J. Chluba, R. Khatri, and R. A. Sunyaev, Mon. Not. R. Astron. Soc. **425**, 1129 (2012).

[64] R. Khatri, R. A. Sunyaev, and J. Chluba, Astron. Astrophys. **543**, A136 (2012).

[65] R. Khatri, R. A. Sunyaev, and J. Chluba, Astron. Astrophys. **540**, A124 (2012).

[66] N. Aghanim *et al.* (Planck Collaboration), arXiv: 1507.02704.

[67] A. Lewis and S. Bridle, Phys. Rev. D **66**, 103511 (2002).

[68] A. Lewis, Phys. Rev. D **87**, 103529 (2013).

[69] M. Cortes, A. R. Liddle, and P. Mukherjee, Phys. Rev. D **75**, 083520 (2007).

[70] D. Baumann, arXiv:0907.5424.

[71] A. A. Starobinsky, Phys. Lett. B **91**, 99 (1980).

[72] Y. B. Zeldovich and R. A. Sunyaev, Astrophys. Space Sci. **4**, 301 (1969).

[73] A. Albrecht *et al.*, arXiv:0901.0721.